AWARD NUMBER: W81XWH-17-1-0137

TITLE: Defining the Consequence of CHD1 Loss on Transcriptional Regulation and Therapeutic Response

PRINCIPAL INVESTIGATOR: Michael A. Augello

CONTRACTING ORGANIZATION: Joan & Sanford I Weill Medical College of Cornell University
New York, NY 10021

REPORT DATE: June 2018

TYPE OF REPORT: Annual

PREPARED FOR: U.S. Army Medical Research and Materiel Command
Fort Detrick, Maryland 21702-5012

REPORT DOCUMENTATION PAGE

Form Approved
OMB No. 0704-0188

1. REPORT DATE	2. REPORT TYPE	3. DATES COVERED
June 2018	Annual	1 Jun 2017 - 31 May 2018

4. TITLE AND SUBTITLE

Defining the Consequence of CHD1 Loss on Transcriptional Regulation and Therapeutic Response

5a. CONTRACT NUMBER

5b. GRANT NUMBER
W81XWH-17-1-0137

5c. PROGRAM ELEMENT NUMBER

6. AUTHOR(S

Michael A. Augello

E-Mail: mia2025@med.cornell.edu

5d. PROJECT NUMBER

5e. TASK NUMBER

5f. WORK UNIT NUMBER

7. PERFORMING ORGANIZATION NAME(S) AND ADDRESS(ES) AND ADDRESS(ES)

Joan & Sanford I Weill Medical College of Cornell University

413 East 69th Street
New York, NY 10021

8. PERFORMING ORGANIZATION REPORT NUMBER

9. SPONSORING / MONITORING AGENCY NAME(S) AND ADDRESS(ES)

U.S. Army Medical Research and Materiel Command
Fort Detrick, Maryland 21702-5012

10. SPONSOR/MONITOR'S ACRONYM(S)

11. SPONSOR/MONITOR'S REPORT NUMBER(S)

12. DISTRIBUTION / AVAILABILITY STATEMENT

Approved for Public Release; Distribution Unlimited

13. SUPPLEMENTARY NOTES

14. ABSTRACT -Genome wide studies have identified a high prevalence of inactivating genomic alterations associated with nucleosome remodeling and modifying enzymes, suggesting that deregulation of chromatin architecture is critical in tumor initiation/progression. CHD1 is a founding member of the chromatin remodeling family, characterized by tandem Chromo-domains, a DNA Helicase domain, and DNA binding domain (CHD1). A multitude of studies have demonstrated that CHD1 is recruited to the promoters of highly transcribed genes by the epigenetic mark H3K4me3, where it redistributes local nucleosomes ahead of RNA polymerase to facilitate efficient transcriptional initiation and RNA processing. While a majority of cell types appear to be dependent upon the function of CHD1, a subclass of primary PCa is characterized by the genomic loss of this chromatin remodeler. Given that PCa is a disease driven by aberrant transcriptional regulation mediated by oncogenic transcriptional factors (e.g. AR and MYC), it is imperative to understand the molecular underpinnings of CHD1 loss in driving these oncogenic programs. For the first time, our preliminary data demonstrate that in a prostate-specific background, CHD1 localizes to enhancer-like regions of the genome specifically occupied by AR and its associated transcriptional regulators (FOXA1 and HOXB13). This CHD1 binding signature is highly consistent with epigenetic marks identifying these enhancer sites, suggesting that CHD1 remodels enhancer-like chromatin to define a unique AR cistrome. Furthermore, CHD1 was found to be dispensable for global transcriptional output in prostate derived models, but was essential for efficient transcriptional processing. Thus, loss of CHD1 may have a global impact on the AR transcriptional network, deregulating both genomic binding and resultant transcriptional output, via distinct molecular mechanisms.

15. SUBJECT TERMS

None provided

16. SECURITY CLASSIFICATION OF:			17. LIMITATION OF ABSTRACT	18. NUMBER OF PAGES	19a. NAME OF RESPONSIBLE PERSON
a. REPORT	b. ABSTRACT	c. THIS PAGE			USAMRMC
Unclassified	Unclassified	Unclassified	Unclassified	17	19b. TELEPHONE NUMBER *(include area code)*

Table of Contents

1: Introduction

PCa is highly dependent upon the action of the androgen receptor (AR), the protein responsible for prostate cell growth and survival at all stages of disease. AR is a transcription factor that is activated by binding to androgens (e.g. testosterone). Activation results in AR binding to DNA where it induces the expression of a specific set of target genes required for prostate development and growth. Importantly, a critical step in the process of prostate tumorigenesis is the rewiring of AR, wherein AR is redirected away from its normal target genes, and instead promotes the expression of genes associated with tumor growth and survival. One well established mechanism for this reprogramming can be seen in the ERG-fusion positive subclass of prostate cancer, which inappropriately expresses the transcription factor ERG. In this context, ERG can physically bind to DNA and AR and direct it to novel sites on DNA, where it forces AR to promote expression of pro-oncogenic genes unique to this subclass of PCa. This signature has been established in a multitude of clinical samples and is distinct from all other subtypes of PCa, including those characterized by CHD1 loss. Thus, while ERG induction has been established as a key event in the rewiring of AR during tumor formation, the mechanisms that alter AR binding in the other subtypes remains unclear.

One such subclass is characterized by the deletion of a specific gene on chromosome 5 called CHD1. It belongs to a family of genes whose primary function is to open up DNA to allow for essential proteins to bind and promote gene expression. Several studies have demonstrated that CHD1 is recruited to genes that are highly expressed and is required to maintain cell survival and growth. Interestingly however, our preliminary data suggests that CHD1 functions differently in a prostate specific setting. For the first time, we demonstrate that in a prostate specific background, 1) CHD1 directs where AR binds to DNA, 2) Cells which lack CHD1 still require AR for growth and survival, 3) Loss of CHD1 does not decrease cell growth or survival, and 4) CHD1 binds to many proteins known to regulate AR function. We thus hypothesize that loss of CHD1 represents a specific mechanism though which AR is reprogrammed to promote tumor formation and growth. Given that the clinical signatures of this subtype of cancer are very distinct from the others, it is likely that identification of the genes that AR regulates in CHD1 deficient tumors will nominate novel pathways that can be targeted to limit growth of this aggressive tumor class.

2: Keywords

- Prostate Cancer
- Androgen Receptor
- CHD1
- Epigenetics
- HOXB13
- Tumor Cistrome
- Prostate Cancer Subclass
- ChIP Sequencing
- AR
- AR signaling
- Tumor Suppressor

3: Accomplishments

Goals:

Overarching goals	Timeline (Months)	Status
AIM 1: Define the Chromatin Landscape upon CHD1 deletion	1-18	In Progress
Generation of cell models	1-3	Completed
ATAC Seq of CHD1 null models	3-5	Optimizing
ChIP Sequencing of CHD1 null models	6-9	Completed
AR RIME of CHD1 null models	6-9	Completed
Analysis of Sequencing data-	10-18	Completed
AIM 2: Describe the impact on transcriptional regulation and tumor biology upon chd1 loss	6-24	In Progress
RNA Seq in CHD1 null models	6-10	Completed
Analysis of RNA Sequencing	11-18	Completed
Correlation with Clinical Data	18-24	Completed
Identify pathways critical for CHD1 null models	12-16	In progress
Assessment of CHD1 null tumor phenotypes	16-24	To begin 7-18
AIM 3: Define CHD1 status as a predictor of therapeutic response	4-24	In Progress
Assessment of CHD1 loss in response to current therapeutic options	4-12	In progress
Novel Drug Screen in CHD1 null models	12-24	To begin 10-18

Accomplishments:

Summary of Accomplishments by Aim

AIM 1: Consequence of CHD1 loss on global chromatin architecture and oncogenic cistromes.

Rationale: There is compelling evidence that CHD1 functions as a potent tumor suppressor in PCa, yet the mechanisms through which this chromatin remodeler limits tumor formation remain unknown. Our preliminary data demonstrate that, in a prostate specific context, CHD1 co-localizes with critical transcriptional regulators at enhancer-like DNA, in patterns consistent with active nucleosome turnover. This suggests that CHD1 acts as a global regulator of chromatin

architecture and transcription factor binding in prostate tissue. Therefore, *Aim1 will build on these findings and define the consequences of CHD1 loss on global chromatin architecture (Aim1A), the cistromes of AR and its co-factors (Aim1B), and the interactome of AR transcriptional complexes (Aim1C).*

Aim 1B: Define the consequence of CHD1 loss on the cistrome of AR and its cofactors.

Methods: Our preliminary data strongly suggests that CHD1 regulates chromatin accessibility at sites enriched for AR and its cofactors. Given the propensity with which CHD1 is lost and human disease, and the well-accepted concept that the AR cistrome is rewired as a function of disease progression, this subaim will characterize the AR cistrome in the absence of CHD1. Utilizing a CRISPR based system, CHD1 was homozygously deleted from human prostate cancer cells (LNCaP-Figure 1) and the AR cistrome assessed after 3 hours of androgen stimulation using ChIP Seq. After initial peak calling using MACS2 and q=0.05, differentially bound AR peaks were defined between CHD1 proficient and deficient models (2 replicates per condition) using the R package Diffbind, with an FDR cutoff of 0.01.

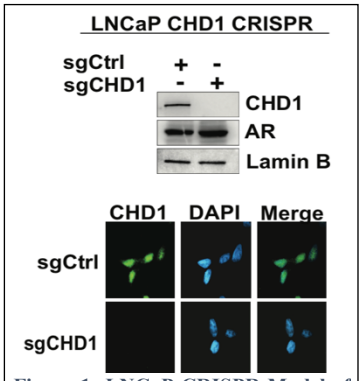

Figure 1: LNCaP CRISPR Model of CHD1 loss. LNCaP cells expressing CAS9 and either a non-targeting or CHD1 specific sgRNA were selected using Puromycin and then blotted for CHD1 and AR (top). A uniform population of CHD1 loss was validted using IF against CHD1 in these isogenic models (bottom).

Results: Significant progress has been made for this subaim. The AR cistrome for CHD1 null PCa cells was defined, wherein nearly 22,000 AR peaks were alternatively bound in the absence of CHD1(Figure 2). These peaks were ~ equally distributed between enhanced and diminished AR binding, with identical distribution across all genomic annotation classes. Importantly, the clinical significance of this alternative (CHD1 null) AR cistrome was validated using AR ChIP Seq from primary human PCa samples. Therein, the tumor-associated AR cistrome mirrored that of our CHD1 null model, with similar patterns of AR binding (enriched at gained sites and diminished at depleted sites) seen across the genome (Figure 2). Further evidence of the relevance and subclass specify of these sites was gained through analysis of H3K27ac ChIP annotated for genomic status. It was seen that CHD1 null tumors harbored elevated levels of this active enhancer mark at gained AR peaks compared to CHD1 WT tumors, with no appreciable difference in its abundance at depleted peaks between genotypes (Figure 2). Thus, these data provide the first evidence for CHD1 as a regulator of nuclear receptor occupancy on chromatin, and identify a novel and clinically relevant AR cistrome in CHD1 deficient prostate tumors.

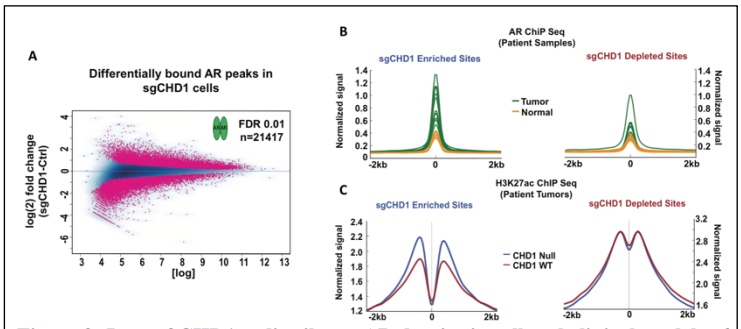

Figure 2: Loss of CHD1 redistributes AR density in cell and clinical models of primary disease. A. MA Plot demonstrating differential peak binding between sgCHD1 and sgCtrl cells in response to androgen stimulation . B. Validation of the CHD1 null AR cistrome in AR ChIP seq datasets derived from primary prostate cancer samples. C. Distribution of the active enhancer histone mark H3K27ac in patient samples segregated based on the genomic status of CHD1.

To better understand the molecular underpinnings of AR rewiring in CHD1 null prostate tumors, motif analyses of the CHD1 null AR cistrome was performed using Homer software and the most updated Jasper Motiff database. Interestingly, the HOXB13 motif was significantly enriched within the gained AR peaks, while AR Half-sites were significantly depleted (Figure 3).

Other factors known to drive alternative AR binding patterns (e.g. FOXA1) were equally present in both datasets, demonstrating that HOXB13 activity may underlie the divergent AR cistrome seen upon CHD1 loss. Indeed, HOXB13 occupancy (ChIP seq) at AR gained sites was significantly enriched in both human PCa tumors and LNCaP models, further demonstrating that the identified motifs are active HOXB13 sites (Figure 3).

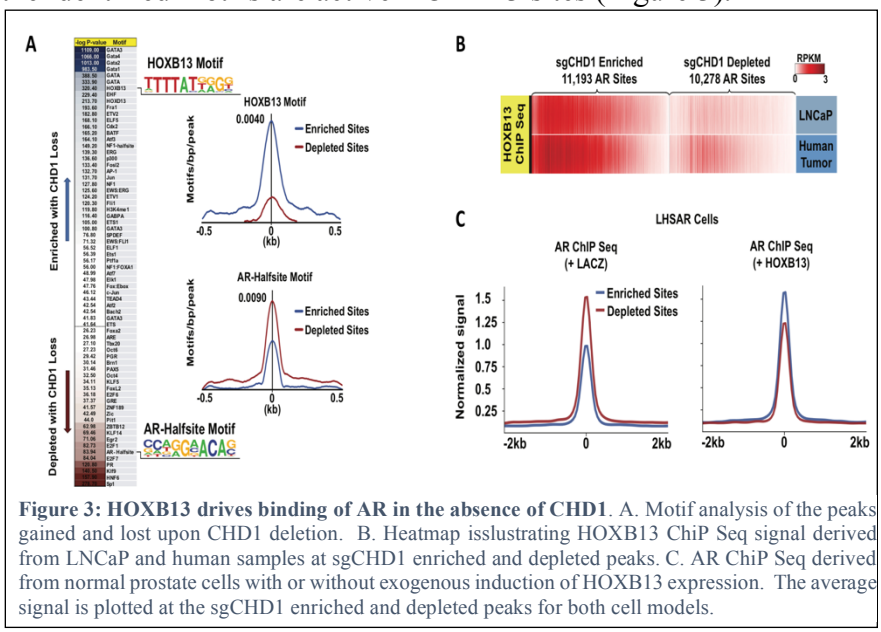

Figure 3: HOXB13 drives binding of AR in the absence of CHD1. A. Motif analysis of the peaks gained and lost upon CHD1 deletion. B. Heatmap isslustrating HOXB13 ChiP Seq signal derived from LNCaP and human samples at sgCHD1 enriched and depleted peaks. C. AR ChiP Seq derived from normal prostate cells with or without exogenous induction of HOXB13 expression. The average signal is plotted at the sgCHD1 enriched and depleted peaks for both cell models.

However, the most compelling evidence implicating HOXB13 as a driver of the CHD1-null AR cistrome was gained through analysis of the AR cistrome in normal prostate cells engineered to express HOXB13. In its absence, AR occupancy anti-correlated with that of the CHD1 null AR cistrome (elevated at depleted peaks and depleted at gained peaks). Importantly, upon HOXB13 induction AR was redistributed across the genome, now positively correlating with AR binding in CHD1 null cells (Figure 3). Collectively, these analyses implicate HOXB13 as a major driver of the CHD1 null AR cistrome, and suggest that HOXB13 binding across the genome is largely CHD1 indifferent.

<u>Aim 1C:</u> Characterize the interactome of AR transcriptional complexes upon CHD1 depletion.

<u>Method:</u> The ability for AR to direct pro-oncogenic programs during disease progression has been associated with changes in the AR interactome on chromatin. Indeed, numerous AR cofactors are known to be differentially expressed in localized disease (e.g. FOXA1, HOXB13, SRC3, etc) which, when complexed with AR, dramatically affect the temporal and kinetic activity of its transcriptional functions. Given our preliminary data which implicate CHD1 activity as requisite for a subset of AR binding across the genome, RIME was performed in our CHD1 null models to determine how the AR interactome changes in the absence of CHD1 nucleosome remodeling activity.

<u>Results:</u> Significant progress has also been made with this subaim. The AR interactome was characterized using RIME in both Ctrl and CRISPR deleted CHD1 LNCaP models (2 replicates/condition). All samples passed the pre-established rigorous quality control criterion, wherein AR itself was in the top 3 proteins identified across all conditions. As a final QC metric, all peptides passing the initial QC filters were run through the CRAPome database to remove common IP and mass spec contaminants. Only peptides with a saint score >= 0.9 were included in the final analysis. Using these datasets, functional validation was performed in the Ctrl AR interactome, which demonstrated a significant enrichment for known AR cofactors (including FOXA1, HOXB13, p300, SMARCA2). This enrichment was confirmed using a metascape-based characterization of the Ctrl AR interactome, listing the AR signaling pathway as the most enriched ontology category within this dataset, and confirming the quality of these data.

Next, a direct comparison was performed between the Ctrl and sgCHD1 AR RIME datasets to define unique or novel complexes formed by AR in the absence of CHD1. Interestingly, a majority of the interactome between the datasets was shared, with less than 10 peptides identified as unique in either case. As an alternative, the relative abundance of all identified peptides was quantified, normalized to total AR signal, and compared between conditions. However, consistent with the previous analysis, the abundance of these identified co-factors was not significantly different between CHD1 proficient and deficient conditions (~90% similarity between samples). While some interesting differences did arise in this analysis (including an enrichment of Beta Catenin in the CHD1 null AR interactome), it can be concluded that there are no major changes to the chromatin bound AR interactome in a CHD1 deficient context, suggesting that the loss of CHD1 impacts AR function upstream of AR cofactor recruitment.

AIM2: Characterize the transcriptional signatures of CHD1 loss and the impact on tumor growth.

Rationale: Our preliminary data demonstrate that, unlike other tissue types, depletion of CHD1 does not decrease total transcriptional output or reduce cell growth, consistent with its proposed role as a tumor suppressor in prostate tissue. Rather, interrogation of the prostate specific cistrome and interactome of chromatin-bound CHD1 uncovered significant enrichment of critical transcriptional regulators, suggesting the tumorigenic consequences of CHD1 loss are manifested through altered transcription factor function and target gene selection. Thus, *the goal of this aim is to identify the oncogenic signatures that result upon CHD1 loss and define transcriptional networks critical to the growth and survival of CHD1 null tumors.*

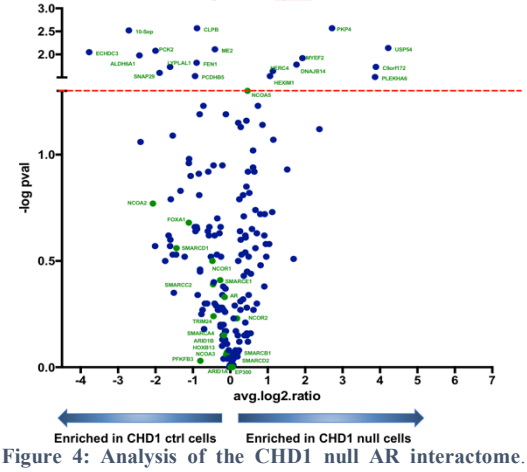

Figure 4: Analysis of the CHD1 null AR interactome. RIME was performed for AR in sgCTRL and sgCHD1 cells after 3 hours of androgen stimulation. Significantly enriched peptides for each conditions were then quantified and differences between conditions plotted as a function of fold change and p-value.

Aim2A: Define the consequence of CHD1 loss on transcriptional control

Method: CHD1 is a known regulator of nucleosome occupancy and transcriptional control, being required for maintenance of numerous lineage specific programs. Thus, loss of CHD1 is likely to have a major impact on transcriptional regulators which control these differentiation pathways. Given the preliminary data which implicates CHD1 as an upstream regulator of AR function, and the knowledge that AR governs luminal differentiation in prostate cells, the consequence of CHD1 loss on AR signaling was assessed in multiple models of CHD1 deficiency using RNA seq.

Results: Initially, human tumors deficient in CHD1 were assessed for AR function within the TCGA dataset using the established AR score as a readout for AR competency. Tumors were binned based upon their genetic status and average AR scores (normalized z-scores) determined for each molecular subclass. Interestingly, CHD1 null tumors displayed an elevated AR-score compared to other established prostate subgroups (i.e ERG and ETS + tumors) (Figure 5). Furthermore, breakdown of the components (genes) which contributed most to the AR score of each subclass uncovered dramatic differences between these groups. The genes that most contributed to the CHD1 null AR score were the ones that contributed the least in other subclasses

(Figure 5). The inverse was also found to be true, wherein the lowest ranked genes within the CHD1 null tumors were some of the highest in the other tumors types, demonstrating that: 1) AR signaling is much more complex than the AR score can report, 2) CHD1 null tumors display a distinct pattern of AR signaling, and 3) more in-depth analyses of AR output are required to understand the subclass specific function of AR in driving pathologic phenotypes.

To validate the findings from TCGA samples, RNA seq derived from LNCaP models of CHD1 loss was conducted in the presence and absence of androgen. These data were then used to derive an AR score for each sample. Consistent with results from above, a dramatic shift in the expression of AR score genes were seen in the absence of CHD1 (Figure 5C). These transcriptional changes tightly correlated with those seen in CHD1 null tumors, as unsupervised clustering of ranked AR score genes clustered CHD1 null LNCaP and CHD1 null tumors away from all other samples (Figure 5D). These findings establish the CHD1 null model as clinically relevant and provide further evidence of alternative AR signaling patterns in CHD1 deficient cells.

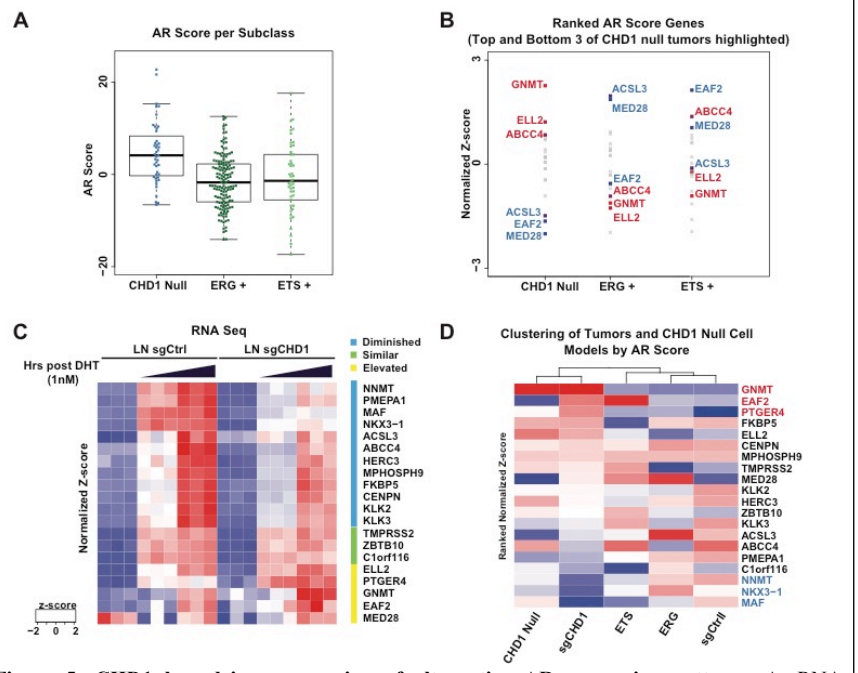

Figure 5: CHD1 loss drives expression of alternative AR expression patterns. A. RNA sequencing (derived from TCGA) was annotated for the genomic status of ERG, ETS, and CHD1 and AR score plotted for each tumor. B. The z-scores for each gene within the AR-score were averaged for each tumor subclass and plotted based on rank. The top 3 (Red) and bottom 3 (Blue) genes which contribute to the CHD1 Null AR score are highlted for each tumor subclass. C. RNA sequencing derived from sgCtrl and sgCHD1 cells stimulated with androgen for 0, 3, or 8 hours. The normalized z-scores of genes comprising the AR score are plotted for each cell model. Genes are clustered based on expression of sgCHD1 cells vs sgCtrl cells at the 8 hour timepoint. D. Normalized z-scores of the AR score genes from the sgCHD1 model are plotted from highest to lowest. The average z-scores from TCGA tumor subclasses and sgCtrl were used to cluster each dataset based on the sgCHD1 ranked list.

Lastly, to more completely define the alternative AR transcription network in CHD1 depleted cells, a CHD1 null AR signature was derived from the sgCHD1 model. Interestingly, this signature encompassed an equal number of induced and repressed genes (compared to time matched Ctrl) and included well-characterized as well as novel AR regulated transcripts (Figure 6B). Importantly, application of this signature to TCGA samples demonstrated high concordance of this signature only within the CHD1 null subclass, with other subtypes showing either discordance or no enrichment for this novel signature (Figure 6C). Finally, GO analysis of KEGG Pathways regulated by this AR transcriptome showed an enrichment for several oncogenic pathways (including AKT) while normal AR-driven prostatic function were consistently depleted (Figure 6D). These data suggest that loss of CHD1 results in a reprogramming of AR, whereby normal prostatic functions are suppressed in favor of pro-oncogenic pathways.

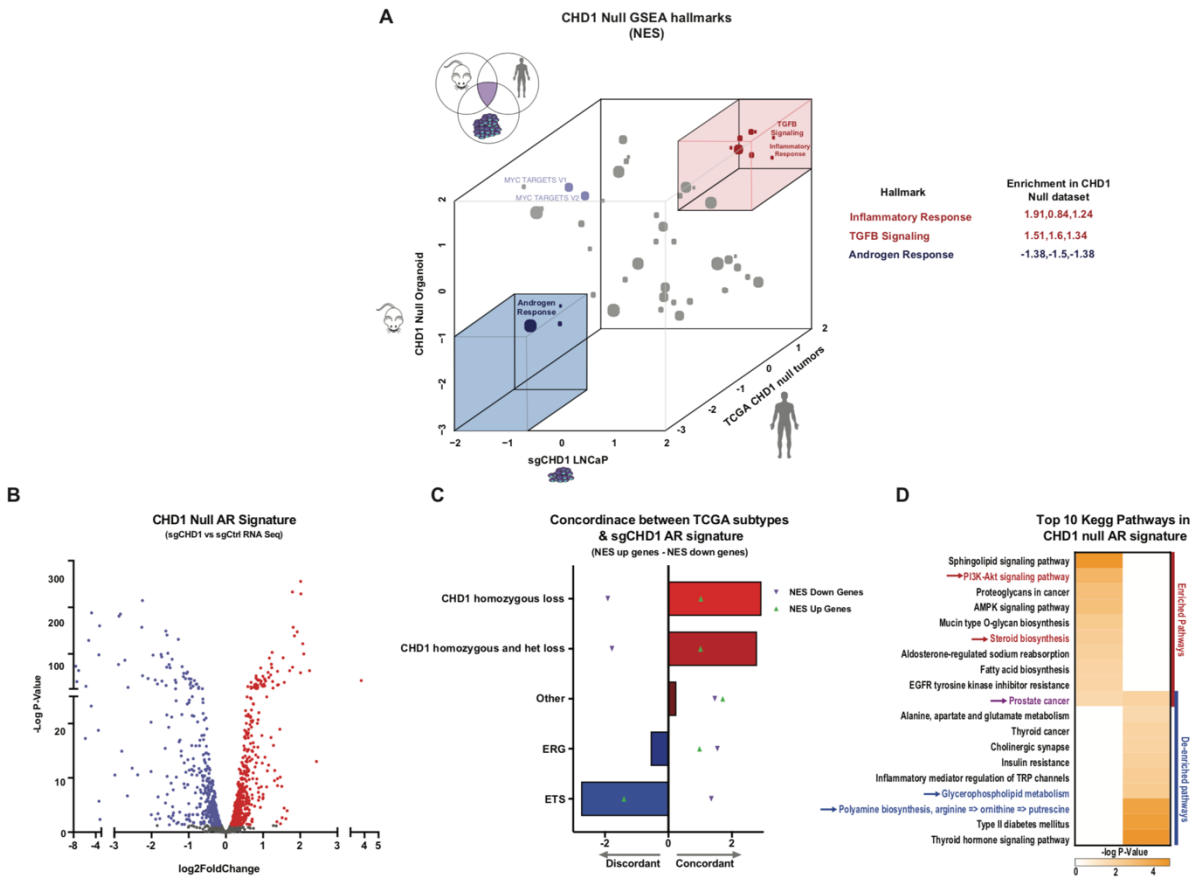

Figure 6: Loss of CHD1 drives a unique AR transcriptome that is associated with activation of oncogenic pathways. A. 3D representation of GSEA Hallmark enrichment utilizing 3 independent datasets deficient in CHD1 expression. *N*ormalized *E*nrichment *S*cores (NES) for all 50 hallmarks were generated for each CHD1 null model (compared to their WT counterparts) and plotted on the X (LNCaP), Y (murine organoid), and Z (human tumors-TCGA CHD1 Null vs CHD1 WT) axes. Hallmarks which demonstrated consistent de-enrichment (Blue) or enrichment (Red) are highlighted in boxes. Gray dots represent hallmarks not consistently enriched between all datasets. Right- Individual NES's for each highlighted hallmark and dataset are shown. **B.** RNA-Seq from LNCaP Ctrl and sgCHD1 cells, starved of hormone for 72 hours and stimulated with 1nM DHT for 8 hours. Differentially regulated transcripts are plotted as a function of log2 fold change and p-value. Red dots-significantly higher, blue dots - significantly lower, gray dots- unchanged transcript abundance in sgCHD1 cells compared to Ctrl. adjusted p-value cutoff 0.05. **C**. Normalized enrichment scores for each TCGA subclass were generated for the upregulated (green up arrows) and downregulated (purple down arrows) genes of the sgCHD1 AR signature. The downregulated NES was subtracted from the upregulated NES and plotted for each TCGA genotype. **D.** KEGG pathways analysis of the induced or repressed transcripts from the sgCHD1 AR signature. The top 10 pathways for each are shown. Highlighted in Red are pathways relevant to PCa progression, while pathways highlighted in Blue are consistent with functions of the normal prostate. Purple is common to both.

Conclusions and Future Goals:

Conclusions for Year 1

- Promoter specific functions of CHD1 are preserved in a prostate specific context
- CHD1 localizes to enhancer-like chromatin enriched for AR and its cofactors
- The enhancer-specific CHD1 interactome is enriched for AR cofactors

Prelim Data

- Loss of CHD1 redistributes AR to sites actively occupied by HOXB13
- The CHD1 null AR cistrome is enriched in the AR cistrome of PCa tumors
- Induction of HOXB13 alone is sufficient to phenocopy the CHD1 null AR cistrome
- CHD1 loss impacts the AR cistrome upstream of cofactor recruitment

Aim 1

- CHD1 null tumors display a unique expression pattern of AR score genes
- The AR score alone is insufficient to accurately assess AR activity across subclasses
- Loss of CHD1 results is a large and divergent AR transcriptome
- The CHD1 null AR signature is concordant with signaling profiles from CHD1 null tumors only
- This signature is enriched for pro-oncogenic pathways & depleted for normal AR-driven prostate functions

Aim 2

Graphical abstract -Year 1 conclusions

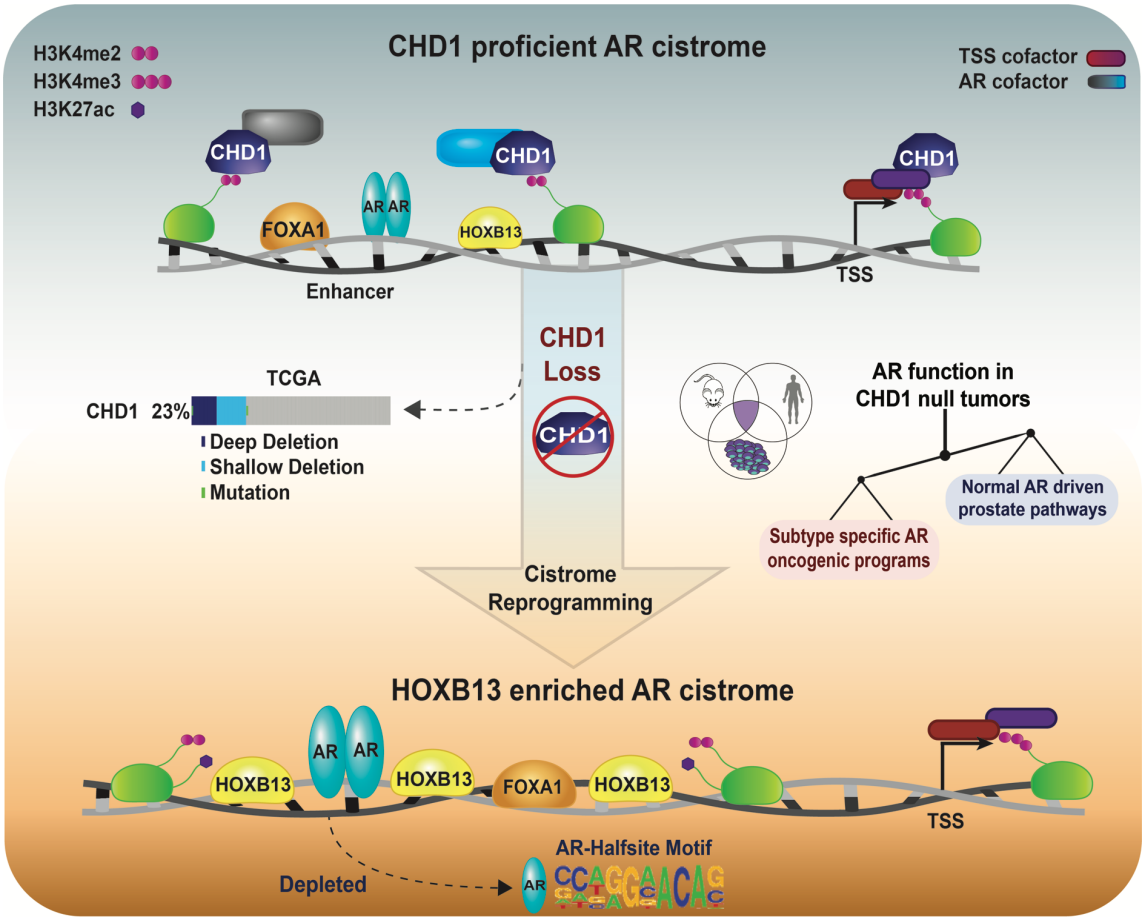

Future Directions:

Aim 1A: Optimize ATAC Seq

1) Optimize conditions to clean up the signal in cell line models
2) Generate novel normalization pipelines to directly compare ATAC signals across samples with varying levels of background

Aim 2B: Define critical pathways required for growth and survival of CHD1 null cells

1) Generate novel model systems utilizing results from Aim1 and Aim 2a
2) Modulate key signaling pathways and delineate the impact on growth and survival in a CHD1 null setting *in vitro* and *in vivo*
3) Nominate critical and/or unique signaling nodes for CHD1 null tumors

Aim 3: Define the response of CHD1 null models to therapeutic intervention

1) Characterize the response of CHD1 null models to AR directed therapeutics
2) Design custom drug panel for large therapeutic screen based on Aims 1, 2 and 3a

Professional Development:

Invited Lectures:

2017	10th Annual Multi-Institutional Prostate Cancer Program SPORE Retreat: "**Defining the impact of CHD1 deregulation on the AR cistrome and PCa progression"** Fort Lauderdale FL
2018	Prostate Cancer Foundation - Genomics/ Genetics/ Epigenetics Webinar Series "**Uncoupling the tumor suppressive and oncogenic functions of CHD1 during prostate tumorigenesis"**

Scientific Presentations:

2017	Prostate Cancer Foundation Retreat "**Consequence of CHD1 loss on cistrome dynamics and prostate cancer progression**" Washington DC, 2017.
2017	AACR Special Conference on Advances in Prostate Cancer Research: **"Consequence of CHD1 loss on cistrome dynamics and prostate cancer progression"** Orlando Florida, December 2-5, 2017
2018	11th Annual Multi-Institutional Prostate Cancer Program SPORE "**Defining the impact of CHD1 loss on AR driven oncogenic programming"** Ft. Lauderdale FL. March 4-6, 2018

Dissemination of Results: Nothing to report

4: Impact

Impact on Principle Discipline: Prostate cancer (PCa) is a highly heterogeneous and lethal disease responsible for a majority of cancer-related deaths in men within the US. Currently, unlike other cancer types, there is a lack of molecular targets available that can help direct therapeutic intervention to thwart disease progression. As such, there is a critical need for the identification and development of novel therapeutic targets to limit cancer growth. Work from our group and others have characterized the genomic landscape of primary PCa and uncovered novel subtypes of

this disease, each encompassing unique chromosomal aberrations, mutations, and transcriptional signatures associated with disease initiation. One of the most common subtypes is characterized by the homozygous loss of the chromatin remodeler CHD1, representing up to 20% of all primary prostate tumors. Interestingly, CHD1 deficiency is highly specific to prostatic tumors, suggesting that this lesion could represent a window for therapeutic intervention. These findings support my objective of defining the consequence of CHD1 loss on transcriptional programs known to drive PCa progression, and nominate molecular pathways that can be targeted to specifically thwart progression of this aggressive subtype. Completion of this proposal has the potential to credential novel molecular targets unique to this subclass, and rapidly translate these findings to the clinic to improve patient mortality and quality of life.

Impact on other Disciplines: Nothing to report

Impact on Technology Transfer: Nothing to report

Impact Beyond Science and Technology: Nothing to report

5: Changes/Challenges

Changes in approach: Nothing to report

Actual or anticipated problems:

Aim 1A: Define the chromatin landscape upon CHD1 loss.

Method: Changes in chromatin architecture and accessibility have recently been associated with the induction of pro-oncogenic programs. Given CHD1 is a well-established member of the nucleosome remodeling family, ATAC seq was performed on human and murine organoid models of CHD1 loss to characterize the chromatin landscape in the context. Furthermore, given the preliminary data implicating CHD1 in the regulation of AR function, these assays were conducted in the presence and absence of physiological doses of androgen. Upon completion, these data will provide critical insight into the prostate specific function of CHD1 in nucleosome remodeling as well as the impact of its loss on AR function.

Run	TotalPeaks	FC>10	FC>20	FRiP	DHS_peaks	DHS_%	Promoter	Exon	Intron	Intergenic
LNCtrlDHT1.rep1	5368	415	39	2.4	4101	82.02	14.1	3.6	38.1	44.2
LNCtrlDHT2.rep1	19601	1839	74	3.9	4268	85.36	13.4	4	40.6	42
LNCtrlEtOH1.rep1	47898	8029	387	7	4550	91	10.5	3.2	43	43.3
LNCtrlEtOH2.rep1	18037	1702	68	3.7	4389	87.78	12.2	3.8	41.7	42.3
LNsgCRSPRDHT1.rep1	60853	15589	963	14.9	4446	88.92	10.2	3.6	43.1	43.1
LNsgCRSPRDHT2.rep1	33167	5316	199	7.2	4487	89.74	12.6	4.2	41.3	42
LNsgCRSPREtOH1.rep1	15147	1630	64	4.2	4478	89.56	15.7	4.5	39.6	40.2
LNsgCRSPREtOH2.rep1	28226	3384	96	5.8	4594	91.88	13.6	4.4	40.7	41.3

Figure 7: QC Results from ATAC seq performed on LNCaP models of CHD1 loss.

Results and future directions: ATAC seq was initially performed in our models using the protocol published in by the Greenleaf group in 2013. However, once run through our established pipeline, it was noted that none of the samples met the pre-determined criteria for peak number or promoter enrichment (2 metrics of WC for ATAC seq data).This was repeated once more with similar results, after which it was determined that the published protocol was toxic to the cell-based models being used. Fortunately, the Greenleaf lab recently published an updated protocol for ATAC Seq, dubbed Omni-ATAC, which is reported to be a universal method to obtain quality ATAC data from a variety of input types (including frozen tissue, stem cells, and cell lines). Thus, this protocol

was employed using the same conditions and models as above. These samples were again run through our standardized pipeline and a significant improvement was seen in the signal to noise ratios compared to previous attempts. Unfortunately, a large degree of variability was detected between replicates for all conditions, disallowing rigorous analysis and subsequent interpretation of the data (Figure 7). Upon discussion with our collaborators within the Elemento Lab (who are experts in ATAC seq prep and analysis), the problems encountered are very common across the field for cell-based models. These difficulties are exemplified by the extreme lack of published ATAC datasets derived from prostate specific models (less than 3 published datasets so far in GEO). Thus, in collaboration with the Elemento lab, we are currently optimizing ATAC conditions as well as developing novel normalization techniques to improve the quality and reproducibility of the ATAC data in prostate tissue. Once successful, these data will not only be useful in defining the consequence of CHD1 loss on global chromatin architecture and transcriptional regulation in PCa, but the optimized protocol will likely prove to be an invaluable resource to the cancer biology field as a whole.

Changes in expenditure, use of animals, or biohazards: Nothing to report

Products: Nothing to report

Participants and other Collaborating Organizations:

Name:	**Michael Augello**
Project Role:	PI
Nearest person months worked	12
Contribution to Project	Designed, performed, and analyzed all experiments for this project
Funding Support:	Department of Defense Post-Doctoral Fellowship Award PC160994

Changes in personnel: Nothing to report

Other Organization Involved: Nothing to report

Cell Line Authentication Service

STR Profile Report

Sample Submitted By:	Weill Medical College of Cornell University Michael Augello
Email Address:	mia2025@med.cornell.edu
ATCC Sales Order:	SO0071335
FTA Barcode:	STRA5295
Cell Line Designation:	LNCaP
Date Sample Received:	Friday, June 22, 2018
Report Date:	Thursday, June 28, 2018

Methodology: Seventeen short tandem repeat (STR) loci plus the gender determining locus, Amelogenin, were amplified using the commercially available PowerPlex® 18D Kit from Promega. The cell line sample was processed using the ABI Prism® 3500xl Genetic Analyzer. Data were analyzed using GeneMapper® ID-X v1.2 software (Applied Biosystems). Appropriate positive and negative controls were run and confirmed for each sample submitted.

Data Interpretation: Cell lines were authenticated using Short Tandem Repeat (STR) analysis as described in 2012 in ANSI Standard (ASN-0002) Authentication of Human Cell Lines: Standardization of STR Profiling by the ATCC Standards Development Organization (SDO) and in Capes-Davis et al., Match criteria for human cell line authentication: Where do we draw the line? Int. J. Cancer. 2012 Nov 8. doi: 10.1002/ijc.27931

ATCC performs STR Profiling following ISO 9001:2008 and ISO/IEC 17025:2005 quality standards.

Technical questions?

ATCC Technical Support
(800) 638-6597 / +1 703-365-2700
tech@atcc.org

Ordering questions?

800-638-6597 or 703-365-2700
Fax 703-365-2750
Email: sales@atcc.org

Cell Line Authentication Service
STR Profile Report

FTA Barcode: STRA5295

ATCC Sales Order: SO0071335

Test Results for Submitted Sample					ATCC Reference Database Profile			
Locus	**Query Profile: LNCaP**				**Database Profile: LNCaP clone FGC; Prostate Carcinoma; Human (Homo sapiens)**			
D3S1358	16							
TH01	9				9			
D21S11	29	32.2						
D18S51	11	12						
Penta_E	12	16						
D5S818	11	12			11	12		
D13S317	10	12			10	12		
D7S820	9.1	10.3			9.1	10.3		
D16S539	11				11			
CSF1PO	10	11			10	11		
Penta_D	12							
Amelogenin	X	Y			X	Y		
vWA	16	18			16	18		
D8S1179	12	14						
TPOX	8	9			8	9		
FGA	19	20						
D19S433	13.2	15						
D2S1338	16							

Number of shared alleles between query sample and database profile:	16
Total number of alleles in the database profile:	16
Percent match between the submitted sample and the database profile:	100

The allele match algorithm compares the 8 core loci plus amelogenin only, even though alleles from all loci will be reported when available.

NOTE: *Loci highlighted in grey (8 core STR loci plus Amelogenin) can be made public to verify cell identity. In order to protect the identity of the donor,* ***please do not publish*** *the allele calls from all the STR loci tested.*
Electropherograms showing raw data are attached.

Explanation of Test Results
Cell lines with 80% match are considered to be related; i.e., derived from a common ancestry. Cell lines with between a 55% to 80% match require further profiling for authentication of relatedness.

☐ The submitted sample profile is human, but not a match for any profile in the ATCC STR database.

☒ The submitted profile is an exact match for the following ATCC human cell line(s) in the ATCC STR database (8 core loci plus Amelogenin): CRL-1740

☐ The submitted profile is similar to the following ATCC human cell line(s):

☐ An STR profile could not be generated.

Additional Comments:

Submitted sample, STRA5295 (LNCaP), is an exact match to ATCC cell line CRL-1740 (LNCaP clone FGC). ATCC CRL-1740 (LNCaP.FGC), is known as a highly unstable cell line.

e-Signature, Technician:	snicholson 6/28/2018
e-Signature, Reviewer:	Bchase 6/28/2018

Cell Line Authentication Service
STR Profile Report

FTA Barcode: STRA5295

ATCC Sales Order: SO0071335

Addendum: Comparative Output from the ATCC STR Profile Database

% Match	ATCC® Cat. No.	Designation	D5S818	D13S317	D7S820	D16S539	vWA	THO1	AMEL	TPOX	CSF1PO
100	STRA5295	LNCaP	11,12	10,12	9.1,10.3	11	16,18	9	X,Y	8,9	10,11
100	CRL-1740	LNCaP clone FGC; Prostate Carcinoma; Human (Homo sapiens)	11,12	10,12	9.1,10.3	11	16,18	9	X,Y	8,9	10,11

Definitions of terms used in this report:

Peak Area Difference (PAD):
Refers to a heterozygous peak imbalance.
Two alleles at a single locus should amplify in a similar manner; and therefore produce peaks of similar height and area. Peaks which are above threshold (50 rfu) but are not of similar area, within 50% of each other, are referred to as a PAD. Due to their nature cell lines do not amplify in the same manner as a sample taken from a fresh buccal swab. PAD is far more common in cell line samples.

Stutter:
A stutter peak is a small peak which occurs immediately before the true peak. It is defined as being a single repeat unit smaller than the true peak. The stutter peak should be less than 15% of the true peak. The stutter is caused by the polymerase.

+4 Peak:
A +4 is similar to a stutter but occurs immediately after the true peak. A stutter peak should be less than 5% for a homozygous and 10% for a heterozygous.

Below Threshold Peak(s):
Cell lines can produce unusual profiles and occasionally a peak will amplify poorly and be below threshold. Where we find a below threshold peak which we believe is valid we indicate it as a below threshold peak. Our cell line analysis criteria, Homozygous and Heterozygous peaks must be equal to or above the set height threshold for it to be considered a true peak.

Ladder/ Off Ladder Peak(s):
The allelic ladder consists of most or all known alleles in the population and allows for precise assignment of alleles. Those which do not align are termed ‘off ladder.

Artifact:
A non-allelic product of the amplification process, an anomaly of the detection process, or a by-product of primer synthesis

Pull-up:
A term used to describe when signal from one dye color channel produces artificial peaks in another, usually adjacent, color.

Spike:
An extraneous peak resulting from dust, dried polymer, an air bubble, or an electrical surge.

Dye blob:
Free dye not coupled to primer that can be injected into the capillary (A known and documented dye blob is often found at the D3S1358 locus.)